JB
Journals.ASM.org

A Conserved UDP-Glucose Dehydrogenase Encoded outside the *hasABC* Operon Contributes to Capsule Biogenesis in Group A *Streptococcus*

Jason N. Cole,[a,b] Ramy K. Aziz,[c,d] Kirsten Kuipers,[a,g] Anjuli M. Timmer,[a] Victor Nizet,[a,e,f] and Nina M. van Sorge[a,g]

Department of Pediatrics, University of California San Diego, La Jolla, California, USA[a]; The School of Chemistry and Molecular Biosciences and the Australian Infectious Diseases Research Centre, The University of Queensland, St. Lucia, Brisbane, Queensland, Australia[b]; Systems Biology Research Group, University of California San Diego, La Jolla, California, USA[c]; Department of Microbiology and Immunology, Faculty of Pharmacy, Cairo University, Cairo, Egypt[d]; Skaggs School of Pharmacy and Pharmaceutical Sciences, University of California San Diego, La Jolla, California, USA[e]; Rady Children's Hospital, San Diego, California, USA[f]; and University Medical Center Utrecht, Utrecht, The Netherlands[g]

Group A *Streptococcus* (GAS) is a human-specific bacterial pathogen responsible for serious morbidity and mortality worldwide. The hyaluronic acid (HA) capsule of GAS is a major virulence factor, contributing to bloodstream survival through resistance to neutrophil and antimicrobial peptide killing and to *in vivo* pathogenicity. Capsule biosynthesis has been exclusively attributed to the ubiquitous *hasABC* hyaluronan synthase operon, which is highly conserved across GAS serotypes. Previous reports indicate that *hasA*, encoding hyaluronan synthase, and *hasB*, encoding UDP-glucose 6-dehydrogenase, are essential for capsule production in GAS. Here, we report that precise allelic exchange mutagenesis of *hasB* in GAS strain 5448, a representative of the globally disseminated M1T1 serotype, did not abolish HA capsule synthesis. *In silico* whole-genome screening identified a putative HasB paralog, designated HasB2, with 45% amino acid identity to HasB at a distant location in the GAS chromosome. *In vitro* enzymatic assays demonstrated that recombinant HasB2 is a functional UDP-glucose 6-dehydrogenase enzyme. Mutagenesis of *hasB2* alone slightly decreased capsule abundance; however, a Δ*hasB* Δ*hasB2* double mutant became completely acapsular. We conclude that HasB is not essential for M1T1 GAS capsule biogenesis due to the presence of a newly identified HasB paralog, HasB2, which most likely resulted from gene duplication. The identification of redundant UDP-glucose 6-dehydrogenases underscores the importance of HA capsule expression for M1T1 GAS pathogenicity and survival in the human host.

The Gram-positive bacterial pathogen *Streptococcus pyogenes*, commonly referred to as group A *Streptococcus* (GAS), is the etiologic agent of numerous human diseases. Clinical manifestations range from benign skin infections, such as impetigo and pharyngitis (~700 million cases per year worldwide), to potentially life-threatening invasive infections, including necrotizing fasciitis and streptococcal toxic shock-like syndrome (~650,000 cases per year worldwide), with an associated mortality of 25% (9). Serious postinfectious sequelae, including acute poststreptococcal glomerulonephritis and rheumatic fever, may also develop following recurrent GAS infections. The resurgence of severe invasive GAS diseases over the past 30 years (10) correlates with the isolation of the globally disseminated serotype M1T1 GAS.

GAS strains express an assortment of surface-associated molecules that contribute to pathogenesis, including a high-molecular-mass hyaluronic acid (HA) capsule consisting of a polymer of alternating glucuronic acid and β-1,3-linked *N*-acetylglucosamine residues (34). The capsule is essentially identical to mammalian HA expressed abundantly on cell surfaces, connective tissue, and the extracellular matrix milieu. The molecular mimicry of host structures enables GAS to avoid detection by the host immune system (14) and accounts for the poor immunogenicity of the GAS capsule in humans (27). A primary role of HA capsule is to provide a physical barrier that promotes bacterial survival through interference with host immune responses, including antibody access to epitopes on the bacterial surface (21), complement deposition (16), and opsonophagocytosis (7, 16, 26). Also, capsule promotes GAS survival in neutrophil extracellular traps (NETs) through enhanced resistance to cathelicidin antimicrobial peptide LL-37, a major constituent of NETs (11). Consequently, acapsular GAS mutants are sensitive to phagocytic killing in human blood *in vitro* and have reduced virulence in murine models of GAS invasive infection compared with encapsulated wild-type (WT) strains (36, 47–49). In addition to its role in systemic infection, capsular HA binds CD44 on host cell keratinocytes to promote GAS adherence to pharyngeal epithelial cells (40) and contributes to pharyngeal colonization in a mouse model (15). Together, these studies confirm a central role for capsule in GAS pathogenicity.

HA capsule biosynthesis in GAS is coordinated by the ubiquitous and highly conserved *hasABC* operon (13, 22). Hyaluronate synthase (encoded by *hasA*) is a membrane-associated enzyme that forms the linear HA polymer by the alternate addition of *N*-acetylglucosamine and glucuronic acid residues from their respective UDP-sugar precursors (19, 23). UDP-glucose 6-dehydrogenase (encoded by *hasB*) forms UDP-glucuronic acid from UDP-glucose in the presence of NAD (24), while UDP-glucose pyrophosphorylase (glucose-1-phosphate uridylyltransferase; encoded by *hasC*) catalyzes the production of UDP-glucose from glucose-1-phosphate and UTP (12). The *hasABC* operon is tran-

Received 23 July 2012 **Accepted** 3 September 2012
Published ahead of print 7 September 2012
Address correspondence to Nina M. van Sorge, n.vansorge-3@umcutrecht.nl.
Copyright © 2012, American Society for Microbiology. All Rights Reserved.
doi:10.1128/JB.01317-12

Downloaded from http://jb.asm.org/ on June 9, 2015 by Universiteitsbibliotheek Utrecht

scribed as a single mRNA transcript from a promoter located upstream of the first gene in the operon, *hasA* (1, 12), with maximal expression occurring in exponential growth phase (13, 45). The region of −10 to −35 of the *hasABC* promoter plays a central role in determining promoter strength and capsule expression levels in GAS (1).

GAS capsule expression is strongly upregulated in human blood (29, 39), and highly encapsulated, or mucoid, isolates are frequently associated with pharyngeal persistence, acute rheumatic fever, and severe invasive human diseases (32, 41). Capsule is also indispensable for the *in vivo* selection of hypervirulent M1T1 GAS variants harboring mutations within the two-component regulator *covRS* (11), also known as *csrRS* (5, 35). Mutations within *covRS* transcriptionally affect ~10 to 15% of the genes within the GAS genome (28, 43), resulting in enhanced expression of the *hasABC* operon and an array of neutrophil resistance genes (10, 44). Enhanced HA capsule expression concomitantly reduces adherence to keratinocytes, extracellular matrix binding, and biofilm formation (31), preventing the dissemination of hypervirulent *covRS* mutant M1T1 GAS among the human population (31).

Previous reports concluded that HasA and HasB are uniquely required for GAS capsule production (3, 18), while HasC is not essential (3, 19). However, these studies inferred the contribution of HasB to GAS HA production by using either heterologous expression systems or Tn*916* transposon mutants with polar effects on downstream gene expression levels. Here, we targeted the *hasB* gene in serotype M1T1 GAS by precise allelic exchange mutagenesis to directly address the role of HasB in capsule biosynthesis. Our results indicate that HasB is a nonessential enzyme for capsule synthesis in M1T1 GAS. We report the identification and characterization of a novel UDP-glucose 6-dehydrogenase, designated HasB2, which can compensate for a nonfunctional HasB enzyme.

MATERIALS AND METHODS

Bacterial strains and growth conditions. GAS strain 5448, a representative of the globally disseminated serotype M1T1 clone, was isolated from a patient with toxic shock-like syndrome and necrotizing fasciitis (33) and is here designated the wild-type (WT) strain. The isogenic Δ*hasA* insertional mutant of this WT strain was described previously (31). GAS strains were routinely propagated at 37°C on Todd-Hewitt agar (THA) or in liquid cultures of Todd-Hewitt broth (THB) (Hardy Diagnostics) under static conditions. When required, growth medium was supplemented with 5 μg/ml erythromycin (Em) or 2 μg/ml chloramphenicol (Cm). *Escherichia coli* strain BL21 Star (DE3) (Invitrogen) was grown at 37°C on Luria-Bertani (LB) (Hardy Diagnostics) agar with 50 μg/ml kanamycin (Km) or in liquid cultures of LB supplemented with 50 μg/ml Km with orbital rotation at 220 rpm.

Allelic exchange mutagenesis of *hasB*. To construct the precise in-frame allelic exchange mutant of *hasB* (GenBank GeneID 3571024), the upstream and downstream regions of *hasB* were PCR amplified from the WT GAS chromosome using the primer pair hasB-up-for (5′-GGCTCTAGAGGACGCACTGTCTACCAATC-3′) and hasB-up-rev-cat (5′-GGTGGTATATCCAGTGATTTTTTTCTCCATCAATCTCT TCCTCATTAAAA-3′, with a 30-bp 5′ extension matching the 5′ end of the chloramphenicol acetyltransferase [*cat*] gene) and the pair hasB-dn-for-cat (5′-ATCTGCGATGAGTGGCAGGGCGGGGCGTAACCATGT CTTCATCTATAACA-3′, with 30 bp 5′ extension matching 3′ end of the *cat* gene) and hasB-dn-rev (5′-GCCGGATCCCCTCTAATTTCAACAGT TCA-3′). Purified upstream and downstream PCR products, in addition to the *cat* PCR product, were amplified with *Pfu* Ultra II (Stratagene) to yield a fusion product in which *cat* precisely replaced *hasB*. This fusion product was cloned into the temperature-sensitive Em^r plasmid pHY304 (38) and electroporated into the WT strain (17), and the transformants were selected by growth on THA supplemented with 5 μg/ml Em for 2 days at 30°C. Single crossover recombination was selected for by shifting to the nonpermissive temperature (37°C) while maintaining Em selection and was confirmed by PCR. Selective pressure was relaxed by serial passage at 30°C without antibiotics, and double crossovers were identified by screening for a Cm^r Em^s phenotype. The in-frame allelic exchange of *hasB* with *cat* in the GAS chromosome was verified by PCR using *hasB*- and *cat*-specific primers.

Insertional mutagenesis of *hasB2*. Genetic mutation of *hasB2* (GenBank GeneID 3572465) in GAS was performed by PCR amplifying a 445-bp fragment starting from 122 bp downstream of the *hasB2* ATG start codon using primers Forw-XhoI (5′-GCGCTCGAGGCAATCCCCTCTT AAAGAAGCAG-3′) and Rev-BamHI (5′-GCGGGATCCTCGCTTCTG CTTCAGAAGAGCC-3′) (underlining indicates restriction sequences). The fragment was cloned into temperature-sensitive plasmid pHY304 and transformed into the electrocompetent WT or Δ*hasB* strain, and single crossover mutants Δ*hasB2* and Δ*hasB* Δ*hasB*2 were generated following temperature shifting and antibiotic selection (Em^r), as described above. Plasmid integration was confirmed by PCR using primers Forw-XhoI and Rev-confirm (5′-CCGAAAGAAGGATTATTGTGCG-3′). Revertant strains, here designated the Δ*hasB2*$_{R1}$ and Δ*hasB* Δ*hasB2*$_{R1}$ strains, were generated by serial passage at 30°C for 2 days in THB without antibiotic selection, prior to the plating of serial dilutions onto THA and overnight incubation at 37°C. Loss of the integrated plasmid from the chromosome was identified by screening for Em^s colonies. Restoration of the *hasB2* allele was confirmed by the HA capsule assay and PCR using primers Forw (5′-GGCTGGAGACAAGAACTAAAGACT-3′) and Rev-confirm to obtain a 974-bp amplicon.

Cloning and recombinant protein expression. The *hasB2* and *hasB* genes were PCR amplified from the WT GAS chromosome using the primer pair HasB2-F (5′-GGGAATTCATGAAAATTACAGTTGTAG-3′) and HasB2-R (5′-GGGAATTCTTAATCATACTGAAAAATATCA-3′) and the pair HasB-F (5′-GGGAATTCATGAAAATAGCAGTTG-3′) and HasB-R (5′-GGGAATTCCTAGTCTCTATTAAAAATATCTCTAC-3′). Purified PCR products were cloned into the Km^r 6×His tag expression plasmid pET-28b (Merck), transformed into chemically competent *E. coli* BL21 Star (DE3) (Invitrogen), and incubated overnight at 37°C with shaking (220 rpm) in LB broth containing 50 μg/ml Km. The next day, cultures were diluted 1:20 into fresh LB–50 μg/ml Km and grown to an optical density at 600 nm (OD_{600}) of 0.6, and recombinant protein overexpression was induced with isopropyl β-D-1-thiogalactopyranoside (IPTG) at a final concentration of 1 mM for 4 h. Bacteria were pelleted by centrifugation at 3,220 × *g* for 10 min and stored at −20°C prior to UDP-glucose 6-dehydrogenase enzymatic assays.

UDP-glucose 6-dehydrogenase enzymatic assay. UDP-glucose 6-dehydrogenase assays were performed as described previously (42). Following IPTG induction of recombinant protein expression in *E. coli* BL21 Star (DE3) described above, bacterial pellets from 10-ml cultures were resuspended in 1 ml of phosphate buffer (50 mM $Na_2HPO_4 \cdot KH_2PO_4$, pH 7.0). Bacterial cells were mechanically disrupted on ice by sonication with the 550 Sonic Dismembrator (Fisher Scientific) and a microtip probe (20 30-s bursts on setting 4.5, with 30-s rests on ice between bursts). Bacterial debris was pelleted by centrifugation at 13,000 × *g* for 10 min at 4°C, and the supernatant was harvested for use as crude enzyme. The protein concentration of the crude extract was determined using a Bio-Rad detergent-compatible (DC) protein assay kit. Enzymatic assays were performed in 96-well flat-bottom plates (Corning) by adding 5 μl of crude enzyme to 195 μl of 50 mM phosphate buffer ($Na_2HPO_4 \cdot KH_2PO_4$, pH 7.0) containing 33 mM $MgCl_2$, 5 mM dithiothreitol (DTT), 5 mM UDP-glucose (Sigma-Aldrich), and 0.5 mM NAD (Sigma-Aldrich). The reduction of NAD at 340 nm was monitored spectrophotometrically at 37°C using a SpectraMax 250 (Molecular Devices), with measurements taken every 30 s for 1 h. The enzymatic reaction rate was calculated from the initial linear

Downloaded from http://jb.asm.org/ on June 9, 2015 by Universiteitsbibliotheek Utrecht

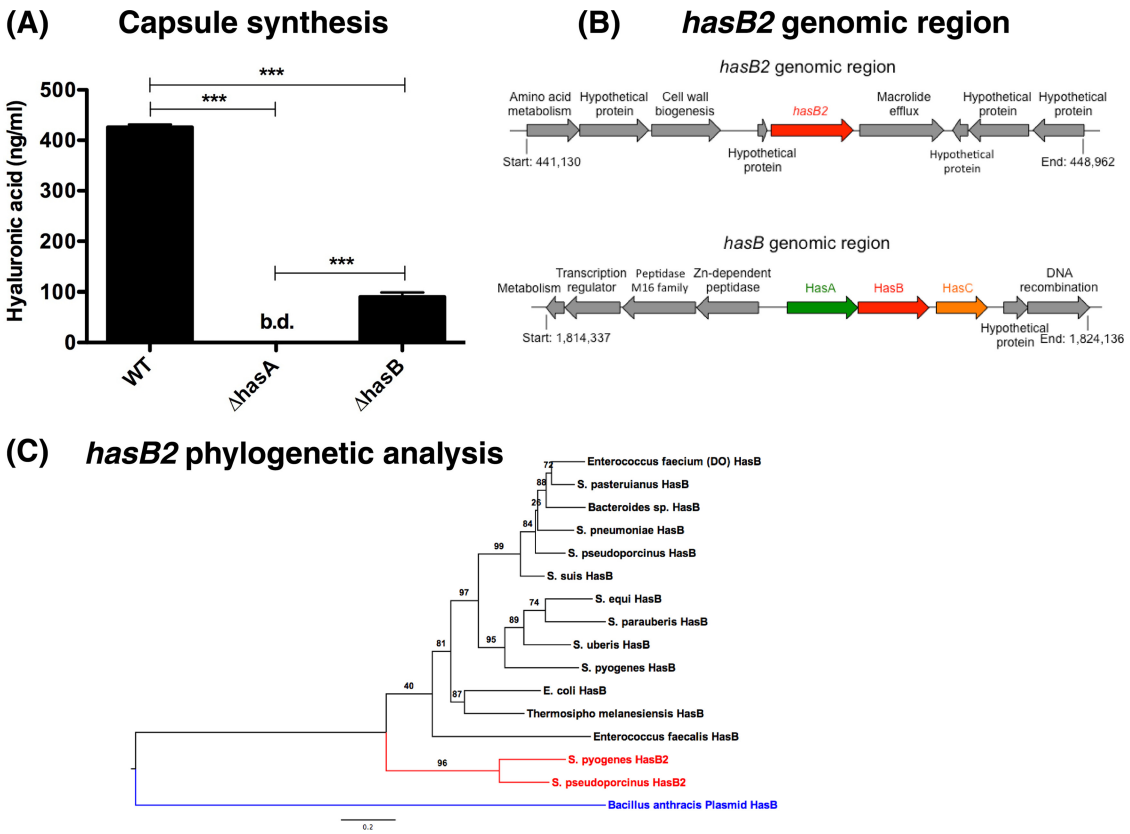

FIG 1 HasB is not essential for capsule production. (A) Quantitation of capsule expression of mid-log-phase M1T1 GAS WT and single *hasA* and *hasB* mutant strains. Data denote the means ± standard errors of the means of pooled data from two independent experiments performed in duplicate. Asterisks indicate values that are statistically significantly different (***, $P < 0.001$). bd, below detection. (B) Genomic organization of the *has* operon and *hasB2* gene, which encodes a putative HasB paralog in M1T1 GAS. Schematic representations of the genomic regions are not drawn to scale. (C) A maximum-likelihood phylogram of HasB2 and a representative set of its homologs indicate a clear distinction between HasB and HasB2. Branch support values are indicated. The plasmid-encoded HasB homolog in *Bacillus anthracis* seems to be equally distant to both paralogs.

portion of the curve (reduction of NAD versus time). The net change in A_{340} per minute (total change − background) was divided by the molar absorptivity of NADH at 340 nm (6,220 M^{-1} cm^{-1}) and the path length (0.6 cm for Costar 96-well flat-bottom plates), multiplied by the reaction volume (2×10^{-6} liters), and then divided by the total protein in the crude enzyme extract (mg). The specific enzyme activity of UDP-glucose 6-dehydrogenase was expressed as micromoles of NADH produced per min per mg of protein.

HA capsule quantification. Two independent assays were used to quantify HA capsule expression in mid-logarithmic-phase cultures. The first method measured cell-associated HA polysaccharide concentration using an HA quantitative test kit (Corgenix), as previously described (31). In the second method, we assessed HA capsule expression by flow cytometry using hyaluronan-binding protein (HABP) (Calbiochem). Bacteria were grown to an OD_{600} of ~0.4, pelleted by centrifugation at 3,220 × *g* for 10 min, and resuspended in HEPES buffer (pH 7.4) containing 5 mM $CaCl_2$, 2.5 mM $MgCl_2$, and 0.1% bovine serum albumin (BSA) ($HEPES^{++}$–0.1% BSA) to an OD_{600} of 0.4 (~1×10^8 CFU/ml). A total of 100 μl of this bacterial suspension was pelleted and stained with biotinylated HABP for 20 min at 37°C under shaking conditions. After samples were washed, they were incubated with phycoerythrin (PE)-conjugated streptavidin (SA) (Jackson ImmunoResearch) for 30 min at room temperature. After a final wash, bacteria were resuspended in $HEPES^{++}$–0.1% BSA and analyzed by flow cytometry. Data represent pooled values from two independent experiments performed in triplicate and normalized to the SA-PE control.

Bioinformatic analyses. The M1T1 theoretical proteome (i.e., all predicted gene products of the M1T1 genome) was searched for similarity to HasA, HasB, and HasC by BLAST-P similarity analysis (2). In addition, the M1T1 GAS genome was rescreened against these three proteins for any potential unannotated proteins by tBLAST-N analysis (2). Operon similarity and chromosomal clustering/colocalization analyses were performed by the Compare Region tool of the SEED database (http://pubseed.theseed.org/seedviewer.cgi) (37). Sequence comparison and phylogenetic analyses were performed on the Phylogeny.FR server (http://www.phylogeny.fr/) (20). Briefly, MUSCLE (25) was used for multiple sequence alignment, PhyML (30) was used for maximum-likelihood phylogenetic distance and branch support value calculations, and, finally, maximum-likelihood phylograms were drawn by FigTree (http://tree.bio.ed.ac.uk/software/figtree).

Superposition of the theoretical HasB2 structure on the resolved three-dimensional (3D) HasB structure (8) was performed using the Cn3D visualization program (46), available at the National Center for Biotechnology Information (NCBI) (http://www.ncbi.nlm.nih.gov/). Functional domains were identified by searches against Pfam database (http://pfam.sanger.ac.uk/). Transmembrane domains were predicted by searching the TMHMM server, version 2.0 (http://www.cbs.dtu.dk/services/TMHMM/). Signal peptide prediction was undertaken using the SignalP, version 4.0, server (http://www.cbs.dtu.dk/services/SignalP/).

Statistical analyses. Capsular expression levels, HABP binding, and UDP-glucose 6-dehydrogenase assays were compared by one-way analysis of variance (ANOVA). Statistical significance was accepted at a *P* value

Downloaded from http://jb.asm.org/ on June 9, 2015 by Universiteitsbibliotheek Utrecht

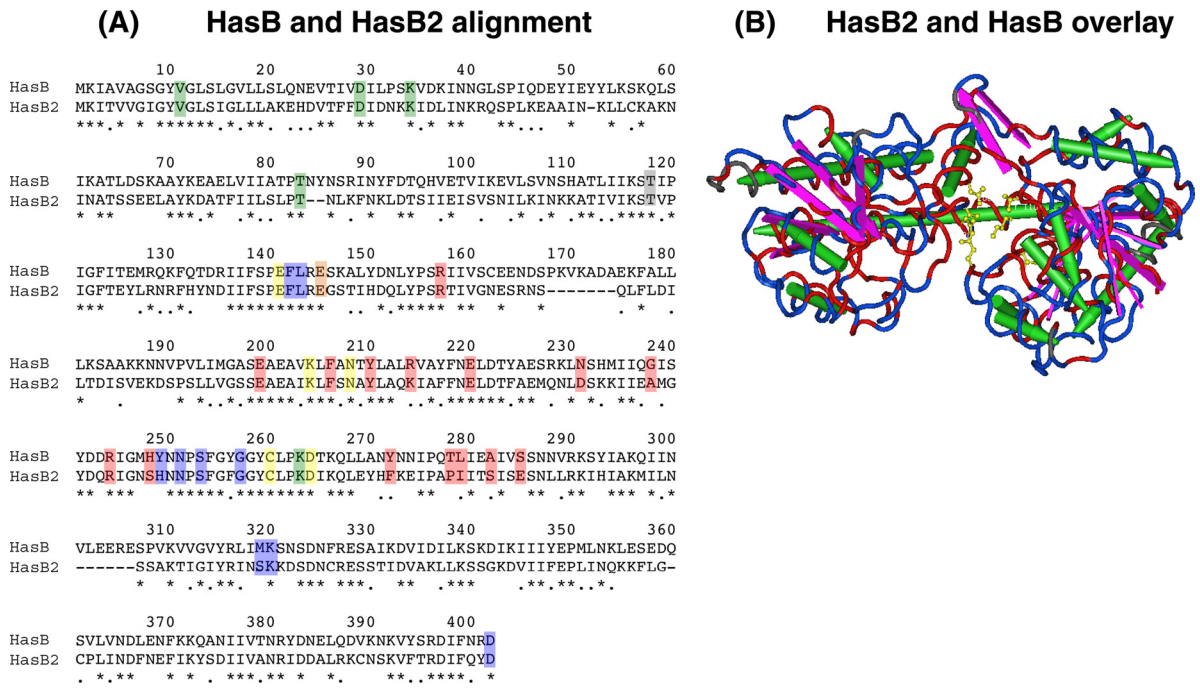

FIG 2 Alignment and 3D overlay of HasB and HasB2. (A) ClustalW alignment of HasB (GenBank GeneID 3571024) and its paralog HasB2 (GenBank GeneID 3572465) from serotype M1T1 GAS strain MGAS5005 (43). HasB2 is 45.3% identical to HasB at the amino acid level. Asterisks denote identical residues; periods indicate similar residues. Residues implicated in catalysis (yellow), NAD(H) hydrogen bonding (green), UDP-sugar binding (blue), and the dimer partner (red) are highlighted. The gray amino acid is implicated in catalysis and NAD(H) hydrogen bonding, while the orange amino acid is implicated in UDP-sugar binding (8). (B) HasB2 is predicted to have structural similarity to HasB. Superposition of HasB2 on the resolved 3D structure of HasB (8) was performed with Cn3D software (46). Sequence conservation is shown as follows: identical residues, red; similar or nonidentical residues, blue). Amino acid residues in the catalytic domain (T118, E141, E145, K204 N208, C260, and D264 of HasB) are indicated in yellow, beta-sheets are in purple, and alpha helices are in green (based on Campbell et al. [8]).

of <0.05. All statistical analyses were performed using GraphPad Prism, version 5.0b (GraphPad Software Inc.).

RESULTS

Capsular expression levels of *hasA* and *hasB* mutants. Previous work reported essential roles for both HasA (hyaluronate synthase) and HasB (UDP-glucose 6-dehydrogenase) in capsule production (3, 18). We set out to verify these findings using individual *has* gene mutants in the genetic background of M1T1 GAS. Compared to the WT, the Δ*hasA* mutant was deficient in cell-associated HA capsule (Fig. 1A), corroborating an essential role for *hasA* in GAS capsule biosynthesis (18). In contrast, precise allelic replacement of the *hasB* gene with the chloramphenicol acetyltransferase (*cat*) gene in the WT M1T1 chromosome reduced, but did not abolish, capsule production (Fig. 1A). These results indicated (i) that *hasB* was not essential for HA capsule synthesis and (ii) that M1T1 GAS must express an additional enzyme with functional UDP-glucose 6-dehydrogenase activity.

Genome-wide screening for a HasB paralog. A previous report on the Has operon of *Streptococcus zooepidemicus* suggested the possibility of a *hasB* paralog in GAS (6). To identify a functional HasB paralog in the M1T1 GAS genome, we used a computational genome-wide screening analysis of published GAS genomes. BLAST-P interrogation of all predicted GAS proteins with the HasB sequence from M1T1 GAS strain MGAS5005 (NCBI protein accession number YP_283215.1) as a query identified a putative UDP-glucose 6-dehydrogenase, designated M5005_Spy0449 (NCBI accession number YP_281812.1), which shares 45.3% amino acid sequence identity with HasB (Fig. 2A). The gene encoding M5005_Spy0449, here designated *hasB2*, consists of 1,158 bp (385 amino acids) and is located in a distinct genomic region ~0.46 Mbp upstream of the *hasABC* synthesis operon (Fig. 1B). This region is highly conserved among all GAS genome sequences and consists of a small open reading frame (ORF) encoding a hypothetical protein, *hasB2*, and a *mefE* homolog encoding a predicted macrolide efflux protein. Interestingly, the extended region surrounding *hasB2* is dissimilar in GAS strains (Fig. 1B) and is disrupted by a short mobile element, with combined phage- and plasmid-like genes (Table 1 and Fig. 1B). Examination of the Atomic Regulon Data, computed from published microarray results (http://pubseed.theseed.org

TABLE 1 The *has* operon and *hasB* paralog genetic locus in different GAS serotypes

Serotype	Representative isolate	Genetic profile					
		hasA	*hasB*	*hasC*	*hasB2*	*mefE*	Contiguous mobile element
M2	MGAS10270	+	Truncated	+	+	+	−
M3	MGAS315	+	+	+	+	+	−
M6	MGAS10394	+	+	+	+	+	−
M12	MGAS2096	+	+	+	+	+	−
M28	MGAS6180	+	+	+	+	+	−
M1	SF370	+	+	+	+	+	+
M1	MGAS5005	+	+	+	+	+	+
M5	Manfredo	+	+	+	+	+	+
M18	MGAS8232	+	+	+	+	+	+
M49	NZ131	+	+	+	+	+	+

Downloaded from http://jb.asm.org/ on June 9, 2015 by Universiteitsbibliotheek Utrecht

TABLE 2 Presence/absence profiles and gene order of members of the *hasABC* and *hasB2* operons in closely related streptococci and other species

Species	*has* operon order	Gene profile (% similarity[a])						Nearby mobile element(s)
		hasA	*hasB*	*hasC*	Short ORF	*hasB2*	*mefE*- like	
S. pyogenes	*hasABC*	+	+	+	+	+	+[b]	Phage/plasmid-like element near *hasB2*
S. equi	*hasABC*	+ (75)	+ (63)	+	−	−	−	
S. uberis	*hasAB. . . hasC*[c]	+ (74)	+ (60)	+	−	−	−	
S. parauberis	*hasAB. . . hasC*[c]	+ (71)	+ (63)	+	−	−	−	
S. pneumoniae	*hasBAC*	+/−[d] (26)	+/−[d] (56)	+/−[d]	−	−	−	Transposon elements around *hasBAC* or *hasB*
S. suis	NA[g]	−	+ (60)	−	−	−	−	Transposon-like elements near *hasB*
Enterococcus faecalis		+ (36)	+ (50)[e]	−	−	+[e]	−	Phage/transposon elements around *hasAB*
S. thermophilus		+ (36)	+ (50)	−	−	−	−	Phage/transposon elements around *hasAB*
Bacillus cereus	*hasACB*	+ (51)	+ (24)	+	−	−	−	Mobile elements or remnants around *hasACB*
Bacillus anthracis	*hasACB*	+ (58)	+ (24)[f]	+	–	+[f]	−	Mobile elements or remnants around *hasACB*
S. pseudoporcinus	NA	−	+ (57)	+	+	+ (67)	+	
Bacillus halodurans		−	−	−	−	+ (48)	−	
Exiguobacterium sibiricum		−	−	−	−	+ (49)	−	

[a] Percent similarity of homologs was calculated on the amino acid levels.
[b] Only if present next to *hasB2*.
[c] *hasC* is not adjacent to *hasB* but the genes are separated by only three ORFs.
[d] *hasB* and *hasA* are present next to *hasC* in some strains while in others *hasB* and *hasC* seem to be separated, and *hasA* is absent.
[e] The *E. faecalis* version of HasB is also 43% similar to HasB2.
[f] The *B. anthracis* HasB is 26% similar to *S. pyogenes* HasB2.
[g] NA, no operon or genes are not contiguous.

/seedviewer.cgi?page = AtomicRegulon&genome = all), indicates that the three genes (the ORF, *hasB2*, and *mefE*) tend to be coexpressed in GAS under various conditions, suggesting that they may form one operon. In addition, *hasB2* transcription is unchanged in *covRS* mutants (data from reference 4), suggesting that *hasB2* expression may not be under regulation by the CovRS two-component system.

The *hasB* and *hasB2* genes are ubiquitous and highly conserved among GAS strains (Table 1); however, *hasB2* was not detected in other streptococcal or enterococcal species, except for *Streptococcus pseudoporcinus* (Table 2). On the other hand, *hasABC* is conserved in many streptococci and still present in some bacilli (Table 2), although in a different order (*hasACB*). Phylogenetic analyses demonstrate that *hasB* is well conserved in bacteria across the phylogenetic tree, including *E. coli*, *Enterococcus*, and some streptococci (Fig. 1C). The *hasB2* gene is distinct from *hasB* genes (Fig. 1C), suggesting that *hasB2* arose as a result of gene duplication in GAS or was acquired by horizontal gene transfer, possibly from *S. pseudoporcinus* or another unsequenced bacterial strain or species.

The predicted size for HasB2 is 43.4 kDa, which is in good agreement with the SDS-PAGE size estimate following T7 overexpression of *hasB2* in *E. coli* (~42 kDa) (data not shown). HasB2 lacks putative signal peptides and transmembrane domains, similar to HasB (data not shown). Interrogation of the Pfam (version 26.0) database reveals that HasB2 and HasB share three distinct UDP-glucose/GDP-mannose dehydrogenase family domains, with predicted active-site residues at C250 and C260, respectively (Table 3) (Fig. 2A). Finally, computational 3D alignments show structural similarities for HasB2 and the published crystal structure of HasB (8) (Fig. 2B), including full conservation of the catalytic residues.

HasB2 UDP-glucose 6-dehydrogenase activity. To account for M1T1 GAS HA capsule production in the absence of a functional HasB enzyme, we hypothesized that *hasB2* encodes a UDP-glucose 6-dehydrogenase. To test this hypothesis, the *hasB2* and *hasB* genes from WT GAS were produced as recombinant proteins in *E. coli* BL21 Star (DE3), and whole-cell lysates were assayed for UDP-glucose 6-dehydrogenase activity. *E. coli* cell extracts harboring the HasB2 and HasB expression plasmids have detectable UDP-glucose 6-dehydrogenase enzymatic activity after IPTG induction, compared to the plasmid-only control (Fig. 3). These data demonstrate that *hasB2* encodes a functional UDP-glucose 6-dehydrogenase.

Capsular expression levels of *hasB2* mutants. We constructed *hasB2* mutants in WT (yielding a Δ*hasB2* strain) and Δ*hasB* (yielding a Δ*hasB* Δ*hasB2* strain) strains to determine whether HasB2 contributes to capsule synthesis in M1T1 GAS. Capsule expression

TABLE 3 Pfam comparisons of HasB2 and HasB amino acid domains

Family name (accession no.)[a]	Description	Amino acid region (E value)[b]	
		HasB2	HasB
UDPG_MGDP_dh_N (PF03721)	UDP-glucose/GDP-mannose dehydrogenase family, NAD binding domain	1–174 (4.5e−39)	1–174 (2.6e−47)
UDPG_MGDP_dh (PF00984)	UDP-glucose/GDP-mannose dehydrogenase family, central domain	187–279 (2.6e−25)[c]	197–290 (2.1e−26)[d]
UDPG_MGDP_dh_C (PF03720)	UDP-glucose/GDP-mannose dehydrogenase family, UDP binding domain	297–383 (1.3e−09)	313–401 (2.8e−11)

[a] Pfam database.
[b] Start residue and end residue are indicated.
[c] Predicted active-site residue, C250.
[d] Predicted active-site residue, C260.

Downloaded from http://jb.asm.org/ on June 9, 2015 by Universiteitsbibliotheek Utrecht

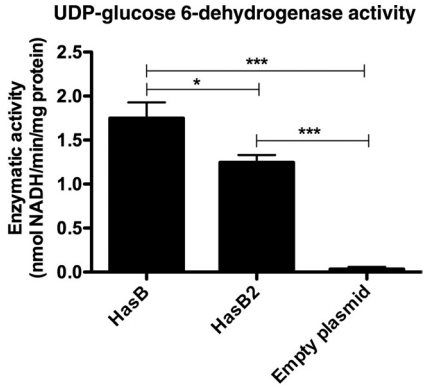

FIG 3 HasB2 is a functional UDP-glucose 6-dehydrogenase. Whole-cell lysates containing recombinant HasB and HasB2 were positive for UDP-glucose 6-dehydrogenase activity, compared to the plasmid-only control, as measured spectrophotometrically by the reduction of NAD at 340 nm. Data represent the means ± standard errors of the means of pooled data from two independent experiments performed in triplicate. *, $P < 0.05$; ***, $P < 0.001$.

levels were analyzed by HA-specific enzyme-linked immunosorbent assay (ELISA) (Fig. 4A). The Δ*hasB2* mutant exhibited reduced capsule production compared to the WT but had levels significantly higher than either the Δ*hasA* or Δ*hasB* strain (Fig. 4A). However, HA synthesis was abolished in the Δ*hasB* Δ*hasB2* double mutant (Fig. 4A), suggesting that *hasB2* can contribute to capsule synthesis, albeit at a reduced level compared to *hasB*. Revertant Δ$hasB2_{R1}$ and Δ*hasB* Δ$hasB2_{R1}$ strains expressed capsule levels equivalent to those of the WT and Δ*hasB* strains, respectively, confirming that the mutations were specific for *hasB2* (Fig. 4A). Flow cytometric analysis with biotinylated HA-binding protein (HABP) revealed that the acapsular Δ*hasA* strain and Δ*hasB* Δ*hasB2* strain bound reduced levels of HABP, compared to the WT, Δ*hasB*, and Δ*hasB2* strains (Fig. 4B), verifying that the Δ*hasB* Δ*hasB2* strain is capsule deficient. Overall, these data indicate that HasB is not essential for M1T1 GAS capsule synthesis.

DISCUSSION

GAS is a human pathogen of global significance, causing an array of mild noninvasive and life-threatening invasive infections. The GAS cell surface is bound by a thick layer of HA, a glycosaminoglycan capsule that promotes *in vivo* survival by circumventing recognition by the host immune system (14) and increasing resistance to phagocyte-mediated killing (11, 16, 36, 49). The exact role of HasB, a UDP-glucose 6-dehydrogenase, in GAS HA capsule biosynthesis remains unclear. Here, we demonstrate that HasB is not essential for serotype M1T1 GAS capsule synthesis. Using a combined approach of molecular genetics and bioinformatics, we identify a putative HasB paralog, termed HasB2, and demonstrate that this protein exhibits UDP-glucose 6-dehydrogenase activity *in vitro*. To our knowledge, this is the first identification of an enzyme outside the *hasABC* operon with a demonstrated role in GAS capsule biogenesis.

Capsule biosynthesis in GAS is coordinated by the universal and highly conserved *hasABC* synthase operon (13, 22), originally identified by Dougherty and van de Rijn through Tn*916* transposon mutagenesis of encapsulated serotype M18 GAS (22). Consistent with previous findings (3, 19), we report that mutagenesis of *hasA* abolishes HA capsule expression in serotype M1T1 GAS. Prior evidence for an essential role of HasB was indirect. For example, Ashbaugh et al. (3) assumed that *hasA* and *hasB* are sufficient for GAS capsule expression based on the observation that *hasC* is not required for capsule synthesis. However, neither targeted mutagenesis nor complementation experiments were performed to corroborate these claims. In addition, previous characterization of acapsular Tn*916*-inactivated transconjugants identified a deficiency in UDP-glucose dehydrogenase enzymatic activity, suggesting a key role for *hasB* in GAS capsule expression (23, 24). However, the lack of UDP-glucose dehydrogenase activity was attributed to a polar effect of Tn*916*::*hasA* mutation on *hasB* expression (23, 24). Finally, insertion of the 16.4-kb Tn*916* element into the chromosome may have disrupted the *hasABC* promoter region at −35 to −10, a major determinant of capsule gene expression levels in GAS (1), impeding expression of the entire *hasABC* operon. Therefore, the precise contribution of *hasB* to capsular HA production in GAS remained ambiguous.

Here, we derived a precise *hasB* allelic exchange mutant in a strain representative of the globally disseminated M1T1 serotype (10). The Δ*hasB* mutant capsular expression levels were reduced compared to the level in WT M1T1 GAS, but the levels were sig-

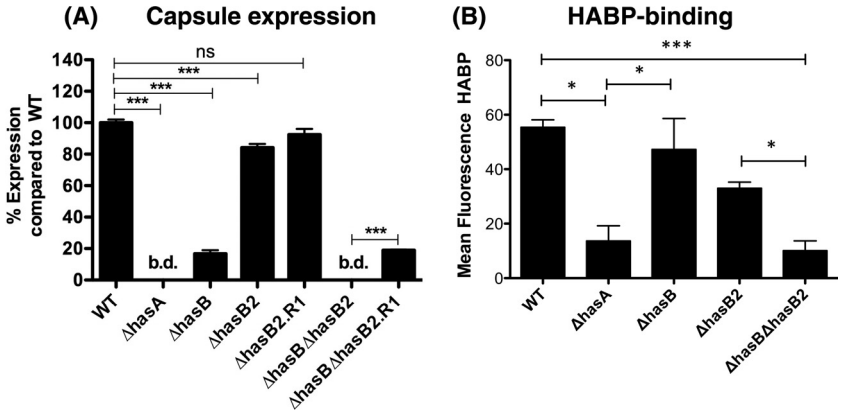

FIG 4 HasB2 contributes to GAS capsule biogenesis. (A) Quantitation of capsule expression in the WT, mutant, and revertant strains propagated to mid-log phase using ELISA (A) and flow cytometric analysis (B) using hyaluronan-binding protein (HABP). ELISA data represent the means ± standard deviations of pooled normalized data from two independent experiments performed in duplicate. Flow cytometry data represent means ± standard deviations of two independent experiments. Asterisks indicate values that are statistically significantly different: *, $P < 0.05$; ***, $P < 0.001$. bd, below detection.

Downloaded from http://jb.asm.org/ on June 9, 2015 by Universiteitsbibliotheek Utrecht

nificantly higher than in the acapsular Δ*hasA* mutant. In contrast to previous studies (3, 19), these data prove that *hasB* is not essential for capsule production in serotype M1T1 GAS. We hypothesized that a *hasB* paralog (6) may compensate for a nonfunctional HasB enzyme, thereby providing substrate for capsule biosynthesis in a Δ*hasB* strain. This hypothesis is supported by previous observations where HasA and HasB together could reconstitute HA biosynthesis in acapsular GAS mutants, *Enterococcus faecalis*, and Gram-negative *E. coli* (19). Expression of constructs producing full-length HasA protein and a nonfunctional truncated HasB protein resulted in detectable capsule production in *E. coli* K5, which contains an endogenous UDP-glucose dehydrogenase. These data suggest that the *E. coli* K5 UDP-glucose dehydrogenase may substitute for the nonfunctional streptococcal HasB enzyme (19).

Bioinformatic interrogation of the serotype M1T1 GAS genomic sequence identified a putative HasB paralog, here named HasB2, with 45% amino acid identity to HasB. Expression of *hasB2* in *E. coli* generated a protein of approximately 42 kDa, and whole-cell extracts exhibited similar UDP-glucose 6-dehydrogenase activity to HasB control extracts. These data demonstrate that *hasB2* encodes a hitherto unidentified UDP-glucose 6-dehydrogenase of GAS. The contribution of *hasB2* to M1T1 GAS capsular biogenesis was confirmed by construction and subsequent analysis of *hasB2* mutants. The Δ*hasB2* mutant displayed reduced capsule expression compared to the WT, but more capsule than the Δ*hasB* strain, suggesting that *hasB2* plays a secondary role to *hasB* in capsule synthesis. Nevertheless, *hasB2* does contribute to HA capsule production, as evidenced by the acapsular phenotype of the Δ*hasB* Δ*hasB2* double mutant. Complementation of the single and double *hasB2* mutants restored capsular expression levels to the WT and Δ*hasB* strains, respectively, confirming that the phenotypes are due to specific *hasB2* mutations and not to pleiotropic mutations or polar effects on gene expression levels.

We used two different HABP-based methodologies (ELISA and flow cytometry) to quantify capsule production. The ELISA-based method provided greater sensitivity and a lower background than the flow method. A possible explanation could be that hyaluronic acid capsule is not covalently attached to the peptidoglycan cell wall and only loosely associated with the bacterial surface. Therefore, during sample preparation for flow cytometric analysis, some capsule may have been lost due to centrifugation at high force during the wash steps, leaving only the tightly associated capsule available for staining and reducing the sensitivity of the assay. In addition, the high background associated with the flow-based method indicates some level of nonspecific HABP binding to intact GAS bacteria, as opposed to results using bacterial extracts in the ELISA method. Overall, the conclusion that can be drawn from these two assays is that *hasB* is not essential for capsule production, despite the differences in the absolute level of contribution.

The bioinformatic and phylogenetic analyses of both the *hasB* and *hasB2* genes and their associated operons (Fig. 1B and C and Table 2) suggest a clear distinction between the evolutionary histories of both paralogs. While *hasB*, often associated with *hasA*, seems to be relatively widespread among streptococci (and has been suggested to have originated from a common streptococcal ancestor [6]), *hasB2* seems to have been more recently acquired and is present in at least two streptococcal species (GAS and *S. pseudoporcinus*). While gene duplication cannot be completely ruled out as the origin of *hasB2*, the similarity between the HasB2 proteins of GAS and *S. pseudoporcinus* is higher than that between HasB and HasB2 within the same species, suggesting lateral transfer rather than intragenomic duplication. Moreover, the fact that *hasB2*, as well as many *hasA* and *hasB* orthologs, is often surrounded by mobile element genes like transposon, phage, or plasmid-like genes (Tables 1 and 2), supports a scenario where those genes are horizontally transferred within and between genomes, perhaps to add functionality to UDP-glucose pyrophosphorylase genes (*hasC* homologs) or provide still undefined biochemical functions. Finally, the presence of *hasA* and *hasB* orthologs on the megaplasmids of *Bacillus cereus* and *Bacillus anthracis* (49) (Table 2), which also carry transposable element genes, even more strongly supports a horizontal origin of these genes.

In summary, we conclude that HasB is a nonessential enzyme for capsular HA expression in serotype M1T1 GAS. A newly identified HasB paralog (HasB2) with functional UDP-glucose 6-dehydrogenase activity has the capacity to support capsule biosynthesis in the absence of a functional HasB enzyme. The identification of an auxiliary UDP-glucose 6-dehydrogenase emphasizes the indispensable role of capsule in GAS pathogenicity and demonstrates the impact of horizontal gene transfer and gene duplication on the evolving virulence potential of microbial pathogens.

ACKNOWLEDGMENTS

J.N.C. was supported by a National Health and Medical Research Council of Australia Overseas Biomedical Training Fellowship (514639) and Project Grant (APP1033258). V.N. was supported by NIH grants AI077780 and AI48176. N.M.V.S. was supported by NIH/UCSD Immunology Training Grant 5T32AI060536.

REFERENCES

1. **Alberti S, Ashbaugh CD, Wessels MR.** 1998. Structure of the *has* operon promoter and regulation of hyaluronic acid capsule expression in group A *Streptococcus*. Mol. Microbiol. **28**:343–353.
2. **Altschul SF, et al.** 1997. Gapped BLAST and PSI-BLAST: a new generation of protein database search programs. Nucleic Acids Res. **25**:3389–3402.
3. **Ashbaugh CD, Alberti S, Wessels MR.** 1998. Molecular analysis of the capsule gene region of group A *Streptococcus*: the *hasAB* genes are sufficient for capsule expression. J. Bacteriol. **180**:4955–4959.
4. **Aziz RK, et al.** 2010. Microevolution of group A streptococci *in vivo*: capturing regulatory networks engaged in sociomicrobiology, niche adaptation, and hypervirulence. PLoS One **5**:e9798. doi:10.1371/journal.pone.0009798.
5. **Bernish B, van de Rijn I.** 1999. Characterization of a two-component system in *Streptococcus pyogenes* which is involved in regulation of hyaluronic acid production. J. Biol. Chem. **274**:4786–4793.
6. **Blank LM, Hugenholtz P, Nielsen LK.** 2008. Evolution of the hyaluronic acid synthesis (*has*) operon in *Streptococcus zooepidemicus* and other pathogenic streptococci. J. Mol. Evol. **67**:13–22.
7. **Boulnois GJ, Roberts IS.** 1990. Genetics of capsular polysaccharide production in bacteria. Curr. Top. Microbiol. Immunol. **150**:1–18.
8. **Campbell RE, Mosimann SC, van De Rijn I, Tanner ME, Strynadka NC.** 2000. The first structure of UDP-glucose dehydrogenase reveals the catalytic residues necessary for the two-fold oxidation. Biochemistry **39**:7012–7023.
9. **Carapetis JR, Steer AC, Mulholland EK, Weber M.** 2005. The global burden of group A streptococcal diseases. Lancet Infect. Dis. **5**:685–694.
10. **Cole JN, Barnett TC, Nizet V, Walker MJ.** 2011. Molecular insight into invasive group A streptococcal disease. Nat. Rev. Microbiol. **9**:724–736.
11. **Cole JN, et al.** 2010. M protein and hyaluronic acid capsule are essential for *in vivo* selection of *covRS* mutations characteristic of invasive serotype M1T1 group A *Streptococcus*. mBio **1**(4):e00191–10. doi:10.1128/mBio.00191-10.

Downloaded from http://jb.asm.org/ on June 9, 2015 by Universiteitsbibliotheek Utrecht

12. **Crater DL, Dougherty BA, van de Rijn I.** 1995. Molecular characterization of *hasC* from an operon required for hyaluronic acid synthesis in group A streptococci. Demonstration of UDP-glucose pyrophosphorylase activity. J. Biol. Chem. **270**:28676–28680.
13. **Crater DL, van de Rijn I.** 1995. Hyaluronic acid synthesis operon (*has*) expression in group A streptococci. J. Biol. Chem. **270**:18452–18458.
14. **Cunningham MW.** 2000. Pathogenesis of group A streptococcal infections. Clin. Microbiol. Rev. **13**:470–511.
15. **Cywes C, Stamenkovic I, Wessels MR.** 2000. CD44 as a receptor for colonization of the pharynx by group A *Streptococcus*. J. Clin. Invest. **106**: 995–1002.
16. **Dale JB, Washburn RG, Marques MB, Wessels MR.** 1996. Hyaluronate capsule and surface M protein in resistance to opsonization of group A streptococci. Infect. Immun. **64**:1495–1501.
17. **Datta V, et al.** 2005. Mutational analysis of the group A streptococcal operon encoding streptolysin S and its virulence role in invasive infection. Mol. Microbiol. **56**:681–695.
18. **DeAngelis PL, Papaconstantinou J, Weigel PH.** 1993. Isolation of a *Streptococcus pyogenes* gene locus that directs hyaluronan biosynthesis in acapsular mutants and in heterologous bacteria. J. Biol. Chem. **268**: 14568–14571.
19. **DeAngelis PL, Papaconstantinou J, Weigel PH.** 1993. Molecular cloning, identification, and sequence of the hyaluronan synthase gene from group A *Streptococcus pyogenes*. J. Biol. Chem. **268**:19181–19184.
20. **Dereeper A, et al.** 2008. Phylogeny.fr: robust phylogenetic analysis for the non-specialist. Nucleic Acids Res. **36**:W465–W469.
21. **Dinkla K, et al.** 2007. Upregulation of capsule enables *Streptococcus pyogenes* to evade immune recognition by antigen-specific antibodies directed to the G-related α2-macroglobulin-binding protein GRAB located on the bacterial surface. Microbes Infect. **9**:922–931.
22. **Dougherty BA, van de Rijn I.** 1992. Molecular characterization of a locus required for hyaluronic acid capsule production in group A streptococci. J. Exp. Med. **175**:1291–1299.
23. **Dougherty BA, van de Rijn I.** 1994. Molecular characterization of *hasA* from an operon required for hyaluronic acid synthesis in group A streptococci. J. Biol. Chem. **269**:169–175.
24. **Dougherty BA, van de Rijn I.** 1993. Molecular characterization of *hasB* from an operon required for hyaluronic acid synthesis in group A streptococci. Demonstration of UDP-glucose dehydrogenase activity. J. Biol. Chem. **268**:7118–7124.
25. **Edgar RC.** 2004. MUSCLE: multiple sequence alignment with high accuracy and high throughput. Nucleic Acids Res. **32**:1792–1797.
26. **Foley MJ, and Wood WB, Jr.** 1959. Studies on the pathogenicity of group A streptococci. II. The antiphagocytic effects of the M protein and the capsular gel. J. Exp. Med. **110**:617–628.
27. **Froude J, Gibofsky A, Buskirk DR, Khanna A, Zabriskie JB.** 1989. Cross-reactivity between streptococcus and human tissue: a model of molecular mimicry and autoimmunity. Curr. Top. Microbiol. Immunol. **145**: 5–26.
28. **Graham MR, et al.** 2002. Virulence control in group A *Streptococcus* by a two-component gene regulatory system: global expression profiling and *in vivo* infection modeling. Proc. Natl. Acad. Sci. U. S. A. **99**:13855–13860.
29. **Gryllos I, et al.** 2001. Regulation of capsule gene expression by group A *Streptococcus* during pharyngeal colonization and invasive infection. Mol. Microbiol. **42**:61–74.
30. **Guindon S, Delsuc F, Dufayard JF, Gascuel O.** 2009. Estimating maximum likelihood phylogenies with PhyML. Methods Mol. Biol. **537**:113–137.
31. **Hollands A, et al.** 2010. Genetic switch to hypervirulence reduces colonization phenotypes of the globally disseminated group A *Streptococcus* M1T1 clone. J. Infect. Dis. **202**:11–19.
32. **Johnson DA, et al.** 2008. High-throughput phenotypic characterization of *Pseudomonas aeruginosa* membrane transport genes. PLoS Genet. **4**:e1000211. doi:10.1371/journal.pgen.1000211.
33. **Kansal RG, McGeer A, Low DE, Norrby-Teglund A, Kotb M.** 2000. Inverse relation between disease severity and expression of the streptococcal cysteine protease, SpeB, among clonal M1T1 isolates recovered from invasive group A streptococcal infection cases. Infect. Immun. **68**:6362–6369.
34. **Kendall FE, Heidelberger M, Dawson MH.** 1937. A serologically inactive polysaccharide elaborated by mucoid strains of group A hemolytic *Streptococcus*. J. Biol. Chem. **118**:61–69.
35. **Levin JC, Wessels MR.** 1998. Identification of *csrR*/*csrS*, a genetic locus that regulates hyaluronic acid capsule synthesis in group A *Streptococcus*. Mol. Microbiol. **30**:209–219.
36. **Moses AE, et al.** 1997. Relative contributions of hyaluronic acid capsule and M protein to virulence in a mucoid strain of the group A *Streptococcus*. Infect. Immun. **65**:64–71.
37. **Overbeek R, Bartels D, Vonstein V, Meyer F.** 2007. Annotation of bacterial and archaeal genomes: improving accuracy and consistency. Chem. Rev. **107**:3431–3447.
38. **Pritzlaff CA, et al.** 2001. Genetic basis for the beta-haemolytic/cytolytic activity of group B *Streptococcus*. Mol. Microbiol. **39**:236–247.
39. **Ravins M, et al.** 2000. Characterization of a mouse-passaged, highly encapsulated variant of group A *Streptococcus* in *in vitro* and *in vivo* studies. J. Infect. Dis. **182**:1702–1711.
40. **Schrager HM, Alberti S, Cywes C, Dougherty GJ, Wessels MR.** 1998. Hyaluronic acid capsule modulates M protein-mediated adherence and acts as a ligand for attachment of group A *Streptococcus* to CD44 on human keratinocytes. J. Clin. Invest. **101**:1708–1716.
41. **Stollerman GH, Dale JB.** 2008. The importance of the group A *Streptococcus* capsule in the pathogenesis of human infections: a historical perspective. Clin. Infect. Dis. **46**:1038–1045.
42. **Stoolmiller AC, Dorfman A.** 1969. The biosynthesis of hyaluronic acid by *Streptococcus*. J. Biol. Chem. **244**:236–246.
43. **Sumby P, et al.** 2005. Evolutionary origin and emergence of a highly successful clone of serotype M1 group A *Streptococcus* involved multiple horizontal gene transfer events. J. Infect. Dis. **192**:771–782.
44. **Sumby P, Whitney AR, Graviss EA, DeLeo FR, Musser JM.** 2006. Genome-wide analysis of group A streptococci reveals a mutation that modulates global phenotype and disease specificity. PLoS Pathog. **2**:e5. doi:10.1371/journal.ppat.0020005.
45. **Unnikrishnan M, et al.** 2002. The bacterial superantigen streptococcal mitogenic exotoxin Z is the major immunoactive agent of *Streptococcus pyogenes*. J. Immunol. **169**:2561–2569.
46. **Wang Y, Geer LY, Chappey C, Kans JA, Bryant SH.** 2000. Cn3D: sequence and structure views for Entrez. Trends Biochem. Sci. **25**:300–302.
47. **Wessels MR, Bronze MS.** 1994. Critical role of the group A streptococcal capsule in pharyngeal colonization and infection in mice. Proc. Natl. Acad. Sci. U. S. A. **91**:12238–12242.
48. **Wessels MR, Goldberg JB, Moses AE, DiCesare TJ.** 1994. Effects on virulence of mutations in a locus essential for hyaluronic acid capsule expression in group A streptococci. Infect. Immun. **62**:433–441.
49. **Wessels MR, Moses AE, Goldberg JB, DiCesare TJ.** 1991. Hyaluronic acid capsule is a virulence factor for mucoid group A streptococci. Proc. Natl. Acad. Sci. U. S. A. **88**:8317–8321.

Downloaded from http://jb.asm.org/ on June 9, 2015 by Universiteitsbibliotheek Utrecht